Agronomy Research **17**(X), xxx–ccc, 2019
https://doi.org/10.15159/AR.19.020

Effects of selected process parameters on the compaction of carob powder

O.L. Akangbe[1,*], J. Blahovec[2], R. Adamovský[1], M. Linda[3] and M. Hromasova[3]

[1]Czech University of Life Sciences, Faculty of Engineering, Department of Mechanical Engineering, Kamycka 129, CZ16521 Praha 6 – Suchdol, Prague, Czech Republic
[2]Czech University of Life Sciences, Faculty of Engineering, Department of Physics, Kamycka 129, CZ16521 Praha 6 – Suchdol, Prague, Czech Republic
[3]Czech University of Life Sciences, Faculty of Engineering, Department of Electrical Engineering, Kamycka 129, CZ16521 Praha 6 – Suchdol, Prague, Czech Republic
[*]Correspondence: akangbe@tf.czu.cz

Abstract. The effects of important process parameters on mechanical response during the densification of an industrial food powder were investigated and important phenomena described using the power rule. The factors studied had highly significant effects on mechanical response. The effects of the models in predicting the behaviour of the system were also highly significant. The findings are of relevance to processing and handling of food powders.

Key words: applied pressure, strain, deformation, compressibility, bulk density.

INTRODUCTION

Important stages during compression or compaction of food powders include particle reorganisation, elimination of fluid components and deformation of solid elements to achieve compact forms (Faborode & O'Callaghan, 1986; Faborode, 1989). These are accompanied by formation of bond bridges and relaxation of the compressed matrix when the applied load is disengaged (Pietsch, 2005; Imole et al., 2014). Several material or equipment and process factors influence mechanical response within the matrix (Laskowski et al., 2005; Wongsiriamnuay & Tippayawong, 2015), some of which interact considerably with one another (Halliday & Smith, 1997). Careful selection of study factors can minimize the size and likelihood of unexplained events (Halliday & Smith, 1997). Uniaxial compression of solid particulates is significantly influenced by the depth of product charge (Divišová et al., 2014) but the effects vary as the capacitive dimensions of the product compression device. The aspect ratio relates depths of charge to diameters of compression gadgets and provides basis for generalising observed effects which may are considered when modelling powder compaction systems. Energy expended during mechanical compaction of food powders is significantly absorbed by the biomaterial as strain (Tomas, 2004; Suescun-Florez et al., 2015). Energy absorption, however, cannot be a function, only, of stress intensity but also a function of the rate at which strain occurs (Russell et al., 2014), which is of direct importance to process efficiency. In uniaxial compression of food materials, the time rate of deformation may

be employed to vary the rate of occurrence of strain (Bagley etal., 1988). In this study, the effects of applied pressure, deformation rate and equipment aspect ratio on mechanical response during the compaction of carob powder were investigated.

MATERIALS AND METHODS

Carob (*Ceratonia siliqua* L.) powder, purchased in Czech Republic, was used for this study. The material had average particle size of 0.5 mm and initial bulk density of 711.69 ± 26.55 kg m^{-3}.

The compression device used is of the form shown in Fig. 1. It consists essentially of a cylindrical die, a base plug and a piston. The die bore diameter was 25 mm and wall thickness was about 40 mm. The base plug is of solid steel, 95 mm in diameter and stepped inwards diametrically, 25 mm from its top, 35 mm from its circumference. The smaller end of the base plug fits closely in the die. A solid piston of 25 mm diameter, 200 mm long compresses the material in the die. The device was mounted on the ZDM 50 universal test rig and loaded compressively through a hemispherical disc.

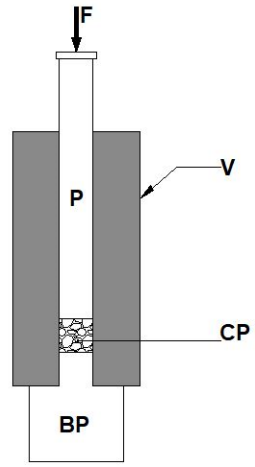

Figure 1. Schematic view of the product compression device showing the base plug, BP, compressed powder, CP, applied load, F, piston, P and cylindrical vessel, V.

Measures of the test powder corresponding to some aspect ratios were fed into the die. The piston was inserted and the device engaged with the load source. Pressure was gradually applied on the material until a maximum value was attained. Two pressure levels were selected as maxima for this study, that is 50 and 100 MPa. The loads were applied at three rates of deformation – 5.5, 10 and 14.5 mm min^{-1}. Three aspect ratios (0.5, 1.0 and 1.5) were also used, being ratios of the depths of material in the die to its bore diameter. These constituted 18 treatments and, in three repetitions, 54 experimental runs – a full factorial concept in a completely randomised design. The tests were conducted under a laboratory condition of 20 °C. Data acquisition was done using the TiraTest software developed by TIRA GmbH, Schalkau, Germany. Sample masses were acquired using the Kern 440–35N (Kern & Sohn GmbH, Stuttgart, Germany) top-loading type weighing balance.

For any treatment condition, a degree of deformation of the compressed material is attained. The highest value of deformation during each test was defined as δ_c (mm). For an established initial depth of product, δ_o (mm) in the compression chamber, the amount of strain induced, ϵ (–), was determined using Eq. 1.

$$\epsilon = \frac{\delta_c}{\delta_o} \tag{1}$$

The rate of strain was obtained as the ratio of this strain to the time required to effect the indicated deformation. The initial bulk density, ρ_b (kg m^{-3}) of the batch of carob powder

used was determined as the mass of the sample of carob powder to the known volume of a cylinder it fills, freely (Mohsenin, 1986). The initial volume of compressed material, v (mm^3) may be determined as (Eq. 2).

$$v = \frac{\pi D^2}{4} \times \delta_O \tag{2}$$

Upon compression, given an internal die diameter, D (mm), compressed material volume, v_c (mm) and a known product mass, m_s (g), the bulk density of the compressed material, ρ_c (kg m^{-3}) may be determined using Eq. 3.

$$\rho_c = \frac{m_s}{v_c} \tag{3}$$

The volume of the compressed product, v_c (mm^3) was calculated using Eq. 4.

$$v_c = \frac{\pi D^2}{4} \times \delta_f \tag{4}$$

where δ_f (mm) – final height of the compressed material in the compression chamber.

The energy required for an indicated amount of deformation may be determined as the area below the force – deformation curve. This was computed numerically by applying the trapezoidal rule (Eq. 5).

$$E = \sum_{n=0}^{n=i-1} \left[\left(\frac{F_{n+1} + F_n}{2} \right) \times (\delta_{n+1} - \delta_n) \right] \tag{5}$$

where n – subdivisions of the deformation axis or incremental deformation, as logged by the test equipment (Akangbe & Herak, 2017); F_N – force required for a deformation, δ_n (mm). With respect to the volume of material compressed, specific energy demand, E_v (J mm^{-3}) may be calculated as follows (Eq. 6).

$$E_v = {}^{E}/_{v} \tag{6}$$

The specific power requirement, $\dot{E}$ is therefore the time rate of expenditure of this energy, determinable using Eq. 7.

$$\dot{E} = {}^{E_v}/_{t} \tag{7}$$

where t – deformation time, s.

Numerical computations and graphical plots were done in MS Excel. Test data were subjected to the analysis of variance using the completely randomised design model in Genstat. Means were compared using Duncan's multiple range test.

RESULTS AND DISCUSSION

The main effects of pressure, deformation rate and aspect ratio on all mechanical response parameters were highly significant ($P < 0.001$), except for the effect of the levels of pressure considered on the rate of strain ($P = 0.493$) and those of the time rate of deformation on specific energy ($P = 0.08$). Significant effects were also observed at the first levels of interaction of the factors studied (Table 1). For instance, except for the effects on deformation and strain, which were not significant ($P = 0.387$ and $P = 0.194$, respectively) the interaction of the time rate of deformation and aspect ratio had highly significant effects ($P < 0.0029$) on all mechanical response parameters. Except for the

rate of strain, no significant effects on response parameters were attributable to the second level of interaction of the parameters studied.

Table 1. Effects of deformation rate and aspect ratio on response variables

Response parameters	Source of variation						
	p	r_d	r_a	$p \times r_d$	$p \times r_a$	$r_d \times r_a$	$p \times r_d \times r_a$
Deformation, δ	0.001**	0.001**	0.001**	0.011*	0.001**	0.387^{ns}	0.028*
Strain, ϵ	0.001**	0.001**	0.001**	0.066^{ns}	0.001**	0.194^{ns}	0.158^{ns}
Strain rate, $\dot{\epsilon}$	0.493^{ns}	0.001**	0.001**	0.901^{ns}	0.658^{ns}	0.001**	0.884^{ns}
Sp. energy, E_v	0.001**	0.08^{ns}	0.001**	0.003	0.001**	0.001**	0.001**
Sp. power, $\dot{E}$	0.001**	0.001**	0.001**	0.001**	0.001**	0.001**	0.349^{ns}
BDCM, ρ_C	0.001**	0.001**	0.001**	0.329^{ns}	0.317^{ns}	0.029*	0.277^{ns}
Gain, G_ρ	0.001**	0.001**	0.001**	0.329^{ns}	0.317^{ns}	0.029*	0.277^{ns}

ns = not significant at the 5% level; * = significant (at the 5% level); ** = highly significant (at the 1% level).

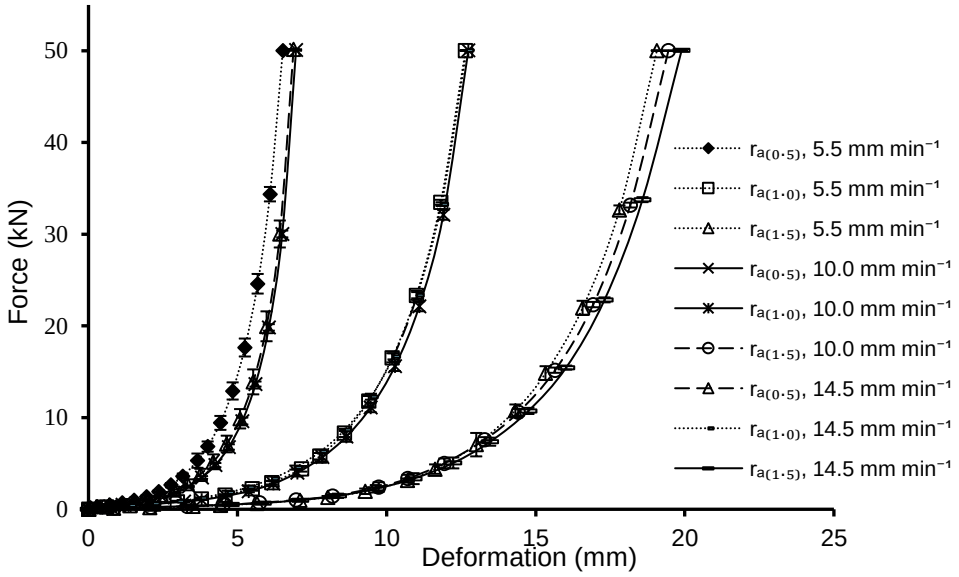

Figure 2. Force – deformation profiles of carob powder at applied pressure of 100 MPa, aspect ratios (r_a) of 0.5, 1.0 and 1.5 and deformation rates of 5.5, 10 and 14.5 mm min^{-1}.

Figure two shows the force–deformation details of compressed powder given a maximum applied pressure of 100 MPa. The profiles are curvilineal, typical of biomaterials (Blahovec, 1982; Yan & Barbosa-Cánovas, 1997). Packing improved with incremental application of compressive load (Raji & Favier, 2004). Higher amount of deformation was occasioned by an increase in pressure from 50–100 MPa (Table 2). The higher the pressure, the higher will be the deformation that may be achieved. Higher rates of deformation resulted in increased deformation. These effects were, however, similar at deformation rates of 10 and 14.5 mm min^{-1} (Table 3). As the aspect ratio increased, deformation also increased (Table 4) and was significantly higher with every increase in the aspect ratio.

More strain was induced at higher pressure (Table 2) and at higher rates of deformation (Table 3); although similar amounts of strain were induced at 10 and 14.5 mm min^{-1}. The highest amount of strain was obtained with the least aspect ratio (Table 4).

Table 2. Main effects of applied pressure on mechanical response parameters

	Applied pressure, p (MPa)	
Response Parameters	50	100
Deformation, δ (mm)	10.5^{b}	11.4^{a}
Strain, ϵ (-)	0.427^{b}	0.465^{a}
Strain rate, $\dot{\epsilon}$ (S^{-1})	0.0045^{a}	0.0081^{a}
Specific energy, E_v (MJm^{-3})	4.70^{b}	4.71^{a}
Power, $\dot{E}$ ($kJm^{-3}S^{-1}$)	49.7^{b}	83.2^{a}
Bulk density of compressed material, ρ_C (kgm^{-3})	1246.0^{b}	1337.0^{a}
Gain in bulk density, G_ρ (%)	75.1^{b}	87.9^{a}

Mean values are compared row-wise. Similar alphabets indicate homogeneous subsets. Significant effects are valid at the 5% level of significance.

Table 3. Effects of the time rate of deformation on mechanical response

	Deformation rate, r_d (mm min^{-1})		
Response Parameters	5.5	10	14.5
Deformation, δ (mm)	11.69^{b}	12.11^{a}	12.21^{a}
Strain, ϵ *(-)*	0.4728^{b}	0.4909^{a}	0.4968^{a}
Strain rate, $\dot{\epsilon}$ (S^{-1})	0.0045^{c}	0.0081^{b}	0.0117^{a}
Specific energy, E_v (MJm^{-3})	6.924^{a}	6.794^{a}	6.924^{a}
Power, $\dot{E}$ ($kJm^{-3}S^{-1}$)	65.6^{a}	108.8^{b}	162.3^{a}
Bulk density of compressed material, ρ_C (kgm^{-3})	1361^{b}	1429^{a}	1416^{a}
Gain in bulk density, G_ρ (%)	90.8^{b}	100.3^{a}	98.5^{a}

Mean values are compared row-wise. Similar alphabets indicate homogeneous subsets. Significant effects are valid at the 5% level of significance.

Table 4. Effects of aspect ratio on mechanical response

	Aspect ratio, r_a (-)		
Response Parameters	0.5	1.0	1.5
Deformation, δ (mm)	6.46^{c}	11.67^{b}	17.88^{a}
Strain, ϵ (-)	0.5170^{a}	0.4667^{c}	0.4767^{b}
Strain rate, $\dot{\epsilon}$ (S^{-1})	0.0132^{a}	0.0066^{b}	0.0044^{c}
Specific energy, E_v (MJm^{-3})	7.35^{a}	6.85^{b}	6.44^{c}
Power, $\dot{E}$ ($kJm^{-3}S^{-1}$)	183.3^{a}	95.2^{b}	58.4^{c}
Bulk density of compressed material, ρ_C (kgm^{-3})	1534^{a}	1374^{b}	1299^{c}
Gain in bulk density, G_ρ (%)	115.0^{a}	92.6^{b}	82.1^{c}

Mean values are compared row-wise. Similar alphabets indicate homogeneous subsets. Significant effects are valid at the 5% level of significance.

Volumetric strain – estimated as axial strain in constrained configurations – may be expressed in direct proportion to increments of pressure (Raji & Favier, 2004). Void capacity is lost progressively, and is strain dependent; there is evidence that this

effect is pulsatile and accounts for two notable phases during compaction (Ozbay & Cabalar, 2016).

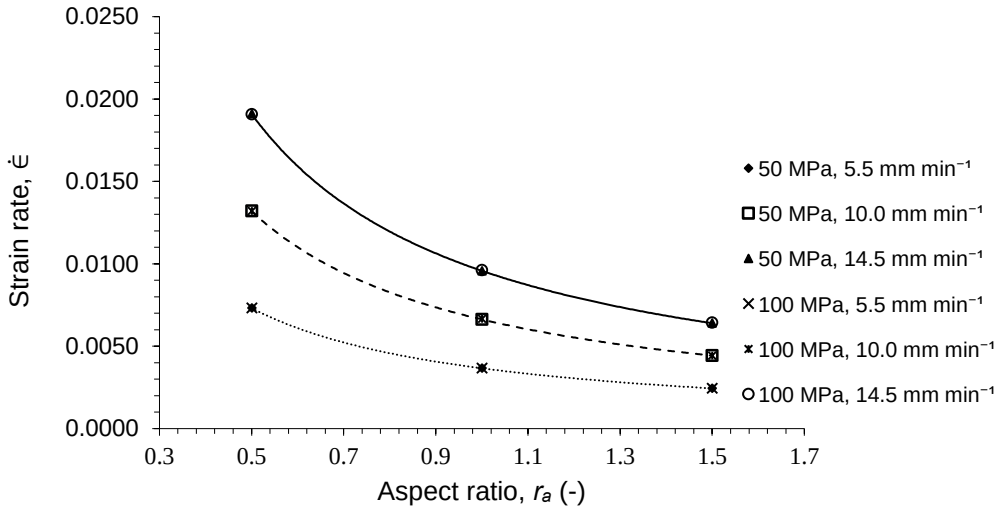

Figure 3. Rates of strain in the compressed powder as functions of the aspect ratio at 50 and 100 MPa and deformation rates of 5.5, 10.0 and 14.5 mm min^{-1}.

Non-recoverable strain is a consistent component of induced strain (O'Dogherty, 1989). Higher rates of strain were occasioned at higher deformation rates and lower aspect ratios (Tables 3 and 4). This relationship is shown in Fig. 3. The rate of deformation is an important determinant of the rate of strain. High rates of strain have been associated with stiffer compacts (Sarumi & Al-Hassani, 1991). The strain rate, $\dot{\epsilon}$ (s^{-1}) may be expressed as a power function of the equipment's aspect ratio, r_a (-), at every level of deformation (Table 5).

$$\dot{\epsilon} = k r_a^n \tag{8}$$

where k – proportionality constant, s^{-1}; n – exponential constant, (-).

Table 5. Estimated parameters of strain rate and specific power as functions of the aspect ratio

Pressure (MPa)	Deformation rate (mm min^{-1})	Strain rate, $\dot{\epsilon}$ (s^{-1})			Specific power, $\dot{E}$ (Jm^{-3}s^{-1})		
		k (s^{-1})	n (-)	R^2	k (s^{-1})	n (-)	R^2
50	5.5	0.0037	-0.9990	1.0000	38.7910	-1.0680	0.9928
	10.0	0.0066	-0.9930	1.0000	66.3140	-1.0880	0.9968
	14.5	0.0096	-0.9960	1.0000	96.5020	-1.1380	0.9967
100	5.5	0.0037	-0.9980	1.0000	64.8650	-1.1430	0.9990
	10.0	0.0066	-0.9930	1.0000	112.1500	-0.9400	0.9970
	14.5	0.0096	-0.9900	1.0000	167.8900	-0.9460	0.9906

Increasing the applied pressure raises energy expenditure (Table 2), as does lowering the aspect ratio (Table 4). Energy demand decreased per unit volume of material compressed as aspect ratio became larger. The time rate of expenditure of energy increased as deformation rate increased (Table 3) and as the aspect ratio was lowered. Specific power requirement is therefore lower at lower rates of deformation

and higher aspect ratios, indicating patterns for energy efficiency during powder compaction. Similar results were reported for related densification systems (Akangbe et al., 2018). There are indications (Mittal & Puri, 2005) that rate dependent compression response is non-linear. Considerable amount of the energy required for compaction is absorbed as plastic deformation (Kulig et al., 2015), translocation of product particles being the dominant initial activity. Fluid pressure builds up within the matrix and is lost, repeatedly over the span of strain. Two positions are reported on fluid pressure build up and loss during uniaxial compression of food materials namely, repeated (Ozbay & Cabalar, 2016) and progressive (Stasiak et al., 2012). A fourth element of energy is responsible for relaxation in the matrix after compaction. Specific power requirement was observed to be a power function of the aspect ratio (Eq. 9), at all rates of deformation (Fig. 4)

$$\dot{E} = kr_a^n \tag{9}$$

where $\dot{E}$ – time rate of expenditure of energy, $\mathrm{Jm^{-3}s^{-1}}$; r_a – aspect ratio, (-); k – constant of proportionality, $\mathrm{s^{-1}}$; n – exponential constant, (-). Parameters of this equation are presented in Table 5, for the different rates of deformation considered. The power law has been used to describe similar relationships such as that between the ratio of in-die to relaxed material density and aspect ratio (O'Dogherty & Wheeler, 1984; Kronbergs et al., 2013).

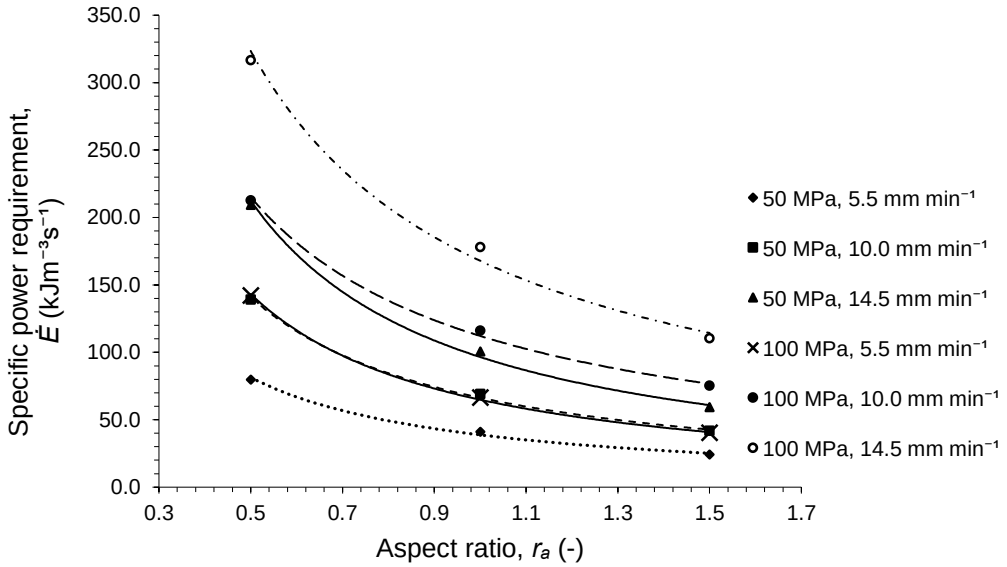

Figure 4. Specific power requirement as a function of the aspect ratio, 50 and 100 MPa of applied pressure and deformation rates of 5.5, 10.0 and 14.5 mm $\mathrm{min^{-1}}$.

The degree of compaction of carob powder was similar at deformation rates of 14.5 and 10.0 mm $\mathrm{min^{-1}}$ but higher than bulk density achieved at 5.5 mm $\mathrm{min^{-1}}$. Applied pressure and aspect ratio were better determinants of gain in bulk density than the time rate of deformation. Bulk density was significantly higher in material compressed at 100 MPa than those compressed at 50 MPa and represented 88% gain at applied pressure of 100 MPa over initial values, compared to gains of 75% at 50 MPa.

Given associated bulk moduli (Johnson et al., 2013), applied pressure considerably determines achievable deformation, with positive correlation to energy requirement for resulting compacts (Adapa et al., 2013). Powder compacted at the least aspect ratio (Table 4) had the highest value of bulk density, which was 1,534 kg m^{-3}. Gains in bulk density increased significantly as aspect ratio was lowered.

CONCLUSIONS

Effects of applied pressure, deformation rate and aspect ratio on mechanical response during the compaction of carob powder were investigated. Main effects of each factor had highly significant effect on mechanical response. Strain rate and specific power requirement were found to be power functions of the aspect ratio at all rates of deformation investigated. Whereas achievable degrees of compaction are higher at lower aspect ratios, energy use efficiency improves with larger aspect ratios. These findings are of direct relevance to processing of food powders into preferred product forms as well as their handling, transport and storage.

ACKNOWLEDGEMENTS. This study was supported by the Integral Grant Agency of the Faculty of Engineering, Czech University of Life Sciences Prague, grant number: 2018: 31130/1312/3119.

REFERENCES

Adapa, P., Tabil, L. & Schoenau, G. 2013. A Comprehensive analysis of the factors affecting densification of barley, canola, oat and wheat straw grinds. *CSBE/SCGAB 2011 Annual Conference* (Vol. 11, p. Paper No. CSBE11-513). Winnipeg, Manitoba.

Akangbe, O. L., Adamovsky, R. & Mosna, F. 2018. Optimising cold compressive recovery of oil from the seeds of Sesame (*Sesamum indicum* L.). *Agronomy Research* **1**6(3), 634–645.

Akangbe, O.L. & Herak, D. 2017. Mechanical behaviour of bulk seeds of some leguminous crops under compression loading. *Scientia Agriculturae Bohemica* **48**(4), 238–244.

Bagley, E.B., Christianson, D.D. & Martindale, J.A. 1988. Uniaxial compression of a hard wheat flour dough: Data analysis using the upper convected Maxwell model. *Journal of Texture Studies* **19**(3), 289–305.

Blahovec, J. 1982. Stlačování upravené žitné slámy [Compaction of modified rye straw]. *Zemědělská Technika* **28**(2), 65–75 (in Czech).

Divišová, M., Herák, D., Kabutey, A., Šleger, V., Sigalingging, R. & Svatoňová, T. 2014. Deformation curve characteristics of rapeseeds and sunflower seeds under compression loading. *Scientia Agriculturae Bohemica* **45**(3), 180–186.

Faborode, M.O. 1989. Moisture effects in the compaction of fibrous agricultural residues. *Biological Wastes* **28**(1), 61–71.

Faborode, M.O. & O'Callaghan, J.R. 1986. Theoretical analysis of the compression of fibrous agricultural materials. *Journal of Agricultural Engineering Research* **35**(3), 175–191.

Halliday, P.J. & Smith, A.C. 1997. Compaction and flow of potato starch and potato granules. *Food Science and Technology International* **3**, 333–342.

Imole, O.I., Paulick, M., Magnanimo, V., Morgeneyer, M., Montes, B.E.C., Ramaioli, M., Kwade, A. & Luding, S. 2014. Slow stress relaxation behavior of cohesive powders. *Powder Technology* **293**, 82–93. http://dx.doi.org/10.1016/j.powtec.2015.12.023

Johnson, P., Cenkowski, S. & Paliwal, J. 2013. Compaction and relaxation characteristics of single compacts produced from distiller's spent grain. *Journal of Food Engineering* **116**(2), 260–266. Retrieved from http://dx.doi.org/10.1016/j.jfoodeng.2012.11.025

Kronbergs, A., Kronbergs, E. & Repsa, E. 2013. Evaluation of reed canary grass shredding and compacting properties. *Agronomy Research* **11**(1), 61–66.

Kulig, R., Łysiak, G. & Skonecki, S. 2015. Prediction of pelleting outcomes based on moisture versus strain hysteresis during the loading of individual pea seeds. *Biosystems Engineering* **129**, 226–236. Retrieved from http://dx.doi.org/10.1016/j.biosystemseng.2014.10.013

Laskowski, J., Łysiak, G. & Skonecki, S. 2005. Material properties in grinding and agglomeration. In J. Horabik & J. Laskowsk (Eds.), *Mechanical properties of granular agro-materials and food powders for industrial practice, Part II* (pp. 47–86). Lublin: Institute of Agrophysics PAS.

Mittal, B. & Puri, V.M. 2005. Rate-dependent elasto-viscoplastic constitutive model for industrial powders. Part 1: Parameter quantification. *Particulate Science and Technology* **23**(3), 249–264.

Mohsenin, N.N. 1986. *Physical properties of plant and animal materials. Vol. I: Structure, physical characteristics and mechanical properties*. New York: Gordon and Breach Science Publishers, pp. 66–76.

O'Dogherty, M.J. 1989. A review of the mechanical behaviour of straw when compressed to high densities. *Journal of Agricultural Engineering Research* **44**, 241–265.

O'Dogherty, M.J. & Wheeler, J.A. 1984. Compression of straw to high densities in closed cylindrical dies. *Journal of Agricultural Engineering Research* **29**(1), 61–72.

Ozbay, A. & Cabalar, A.F. 2016. Effects of triaxial confining pressure and strain rate on stick-slip behavior of a dry granular material. *Granular Matter* **18**(3), 1–9.

Pietsch, W. 2005. *Agglomeration in Industry: Occurrence and Applications*. Weinheim, Germany: WILEY-VCH.

Raji, A.O. & Favier, J.F. 2004. Model for the deformation in agricultural and food particulate materials under bulk compressive loading using discrete element method. I : Theory, model development and validation. *Journal of Food Engineering* **64**, 359–371.

Russell, A., Müller, P. & Tomas, J. 2014. Quasi-static diametrical compression of characteristic elastic-plastic granules: Energetic aspects at contact. *Chemical Engineering Science* **114**, 70–84. Retrieved from http://dx.doi.org/10.1016/j.ces.2014.04.016

Sarumi, M.A. & Al-Hassani, S.T.S. 1991. High and low strain rate properties of powders for continuum analysis. *Powder Technology* **65**, 51–59.

Stasiak, M., Skiba, K., Molenda, M., Tys, J. & Mościcki, L. 2012. The mechanical parameters of rapeseed cake. *Energy Sources, Part A: Recovery, Utilization and Environmental Effects* **34**(13), 1196–1205.

Suescun-Florez, E., Kashuk, S., Iskander, M. & Bless, S. 2015. Predicting the Uniaxial Compressive Response of Granular Media over a Wide Range of Strain Rates Using the Strain Energy Density Concept. *Journal of Dynamic Behavior of Materials* **1**(3), 330–346.

Tomas, J. 2004. Product design of cohesive powders - Mechanical properties, compression and flow behavior. *Chemical Engineering and Technology* **27**(6), 605–618.

Wongsiriamnuay, T. & Tippayawong, N. 2015. Effect of densification parameters on the properties of maize residue pellets. *Biosystems Engineering* **139**, 111–120. Retrieved from http://dx.doi.org/10.1016/j.biosystemseng.2015.08.009

Yan, H. & Barbosa-Cánovas, G.V. 1997. Compression characteristics of agglomerated food powders: Effect of agglomerate size and water activity Caracter & iacute; sticas de la compresi & oacute ; n de. *Food Science and Technology International* **3**, 351–359.